Electron-phonon interaction in one dimension: Exact spectral properties

V. Meden and K. Schönhammer
Institut für Theoretische Physik, Universität Göttingen, Bunsenstraße 9, D-37073 Göttingen, Germany

O. Gunnarsson
Max-Planck-Institut für Festkörperforschung, D-70506 Stuttgart, Germany
(Received 31 May 1994)

One-electron spectral functions for a one-dimensional continuum model including electron-phonon coupling are calculated exactly. The electrons coupled to the phonons represent a Luttinger liquid. Results are presented for an Einstein model for spinless electrons and for the model including spin. Apart from Luttinger-liquid features, the spectra show a rich satellite structure with peak separations partially determined by matrix-element effects. The use of Migdal's approximation neglecting vertex corrections fails to reproduce the exact spectra even for an effective bandwidth large compared to the phonon frequency. The relevance to high-resolution valence photoemission from quasi-one-dimensional conductors is discussed.

Photoemission spectra can be strongly influenced by the electron-phonon coupling. For the case of core levels this is rather well understood as simplified models can be solved exactly.[1,2] An approximate treatment of valence photoemission was presented in a classical paper by Engelsberg and Schrieffer (ES).[3] In the spirit of Migdal's theorem[4] they calculated the single particle Green's function G in the self-consistent Born approximation for an Einstein and a Debye model. For k values corresponding to energy differences to the Fermi energy of the order of the energy of an Einstein phonon ω_0, they found strong deviations from the quasiparticle picture. In their calculation for a three-dimensional (3D) system ES approximated the free electronic density of states by its value at the Fermi surface. The accuracy of the ES one-particle spectra for 3D systems is not easy to estimate, as the calculation of higher order corrections is difficult. In this paper we show that *exact* spectra for the model with a constant density of states can be obtained, by observing that such a density of states occurs in a 1D model with a linearized energy dispersion. This model can be solved exactly by bosonization for arbitrary phonon dispersion ω_q in generalization of the method used for the electron-electron interaction.[5,6] For a Debye model one could alternatively calculate the Green's function using a Ward identity.[7,8] Recent high resolution valence photoemission measurements on quasi-one-dimensional conductors[9] seem to verify the Luttinger liquid picture[6] expected theoretically due to the electron-electron interaction. For a discussion of the low energy spectra of these materials a detailed understanding of the influence of the phonons on the spectra is indispensable. This we provide in the following.

Migdal's theorem is important for the treatment of the electron-phonon coupling in ordinary metals and is a part of the Migdal-Eliashberg theory[10] of superconductivity. Our exact solution presents a clear example of the limited value of the "proof" using low order perturbation theory. The 1D electrons coupled to the phonons represent a Luttinger liquid,[6] which cannot properly be described using Migdal's approximation, which completely neglects vertex corrections.

The transition from spinless electrons to a model including spin does not change the spectra in the self-consistent Born approximation.[3] Our exact spectra, on the other hand, show that there is a *qualitative* difference due to spin-charge separation as it is known from the model with electron-electron interaction.[11–13] The inclusion of both electron-phonon and electron-electron interaction is straightforward using bosonization but will not be discussed here.[14] With this technique one naturally calculates the one particle Green's function $G(x,t)$. To obtain the spectral functions $\rho^{(<)}(k,\omega)$ which determine the photoemission (inverse photoemission) spectra a double Fourier transformation is necessary. This we perform by a generalization of the technique introduced in Ref. 12.

We start from the Hamiltonian

$$\hat{H} = \sum_k \varepsilon_k \hat{c}_k^\dagger \hat{c}_k + \sum_q \omega_q \hat{b}_q^\dagger \hat{b}_q + \sum_{k,q} g(q) \hat{c}_{k+q}^\dagger \hat{c}_k \left(\hat{b}_q + \hat{b}_{-q}^\dagger\right), \quad (1)$$

where $\hat{c}_k$ ($\hat{b}_q$) are the electron (phonon) annihilation operators. As we assume the electron-phonon coupling strength $g(q)$ to be nonzero only for $|q| < q_c$ with $q_c \ll k_F$, we linearize the energy dispersion around the Fermi points, i.e., $\varepsilon_k = v_F(|k| - k_F)$ as in Tomonaga's seminal paper.[15] After bosonizing the electronic degrees of freedom, a canonical transformation reduces the Hamiltonian to a sum of mixed, but independent electron-phonon boson modes[16] with energies $\Omega_{q,1/2}^2 = (v_F^2 q^2 + \omega_q^2)/2 \mp [(v_F^2 q^2 - \omega_q^2)^2/4 + 4\tilde{g}_q^2 v_F q^2 \omega_q]^{1/2}$, where $\tilde{g}_q^2 = (L/2\pi) g^2(q)$ with L the length of the system. In order to calculate the Green's function $G_\alpha(x,t)$, where $\alpha = +,(-)$ denotes the right (left) moving branch of electrons we bosonize the field operators $\hat{\psi}_\alpha(x)$ as in the electron-electron interaction case[5,6] and obtain $G_\alpha(x,t)$

using the eigenvectors of the coupled boson problem. As $\rho_\alpha^>(k_F+\tilde{k},\omega)=\rho_\alpha^<(k_F-\tilde{k},-\omega)$, where ω is measured relative to the chemical potential and $\tilde{k}\equiv k-k_F$, we only calculate

$$iG_+^<(x,t)=\frac{1}{L}e^{ik_Fx}\exp\Big\{\sum_{q>0}\sum_{\nu=1,2}\frac{2\pi}{qL}\times\Big[\left(c_{+,q,\nu}^2e^{-iqx}+c_{-,q,\nu}^2e^{iqx}\right)e^{i\Omega_{q,\nu}t}-2c_{-,q,\nu}^2\Big]\Big\},\tag{2}$$

where

$$c^2_{\substack{+\\(-)},q,\nu}=\frac{\left(v_F|q|_{\substack{+\\(-)}}\Omega_{q,\nu}\right)^2|\Omega_{q,\nu}^2-\omega_q^2|}{4v_F|q|\Omega_{q,\nu}\left(\Omega_{q,2}^2-\Omega_{q,1}^2\right)}.\tag{3}$$

These coefficients obey the "sum rule" $c_{+,q,1}^2+c_{+,q,2}^2-c_{-,q,1}^2-c_{-,q,2}^2=1$.

In the following we restrict ourselves to an Einstein model with q-independent frequency ω_0 and coupling constant $\tilde{g}$ for $|q|<q_c$. The relevant *dimensionless* coupling constant is given by $\beta\equiv\tilde{g}^2/(\omega_0v_F)$. The q dependence of the two boson modes is shown in Fig. 1 for an intermediate coupling strength $\beta=0.1$. The model becomes unstable for the critical coupling strength $\beta_c=0.25$, where the renormalized Fermi velocity $\tilde{v}_F$ given by the slope of $\Omega_{q,1}$ for $q\to0$ goes to zero. In the limit $\omega_0\to\infty$ with $\tilde{g}^2/\omega_0$ and q_c fixed the electron-phonon model corresponds to an *attractive* electron-electron interaction, where this instability is known to occur. In this limit it is therefore obvious that the 1D electron-phonon model is a Luttinger liquid. For arbitrary parameters this follows from general arguments by Haldane[6] and (or) our explicit result Eq. (2) for $G(x,t)$. The anomalous dimension is determined by

$$\lim_{q\to0}c_{-,q,1}^2=\left(\frac{2\beta}{1+\sqrt{1-4\beta}}\right)^2\frac{1}{\sqrt{1-4\beta}},\tag{4}$$

i.e., the leading order is $\beta^2\sim\tilde{g}^4$. If the Green's function is calculated by perturbation theory for the self-energy no indication of Luttinger liquid behavior shows up in the Born approximation $\sim\tilde{g}^2$, which is identical to the self-consistent Born approximation.[3] In order to correctly describe the anomalous dimension perturbatively one needs a resummation of *all* fourth order diagrams (see Fig. 2) including the "non-Migdal" diagram 2(c). The necessity to include this diagram can most simply be seen in a simplified version of the present model with only "right moving" electrons and phonons analogous to the g_4 model in the electron-electron interaction case.[12] In this model omission of diagram 2(c) leads for small negative $\tilde{k}$ to a wrong splitting of the main peak of the spectra in fourth order perturbation theory. An extended discussion of that problem will be given in Ref. 14.

In order to obtain the spectral function $\rho^<(k,\omega)$ a double Fourier transform is necessary. The summation (integration) in the exponent on the rhs of Eq. (2) cannot be performed analytically. An additional problem is given by the slow decay of $G(x,t)$ for large arguments and the singular contribution of the factor presented by the noninteracting Green's function $G^{(0)}(x,t)$. We therefore consider large but finite systems and expand $G(x,t)$ recursively in a Laurent series in $\exp\left(i\frac{2\pi}{L}x\right)$ as in Ref. 12, which allows us to perform the x integration analytically. At this point we have to introduce the cutoff q_c which we usually take much larger than $k_0\equiv\omega_0/v_F$, i.e., the effective bandwidth v_Fq_c is chosen much larger than ω_0. As long as $|k-k_F|\ll q_c$ the resulting spectral functions $\rho_\alpha^<(k,\omega)$ are insensitive to the value of q_c. The time Fourier transform is done numerically with an exponential damping factor $\exp(-\gamma|t|)$, corresponding to a convolution of the spectrum with a narrow Lorentzian. This way the discreteness of the spectra for large but finite systems no longer shows up. For all calculated spectra the sum rule for the total spectral function $\int d\omega\,[\rho_\alpha^<(k,\omega)+\rho_\alpha^>(k,\omega)]=1$ is numerically fulfilled with very high accuracy.

In Fig. 3 we show results for $\rho_+^<(k,\omega)$ for the same coupling strength as in Fig. 1 and various values of the momentum $\tilde{k}$. The corresponding results using second order self-energy (the result of Engelsberg and Schrieffer for finite systems including a Lorentzian broadening) are shown in Fig. 4. The absolute values of the peak positions in the exact spectra in Fig. 3 are indicated in Fig. 1. In order to understand the peak structure the

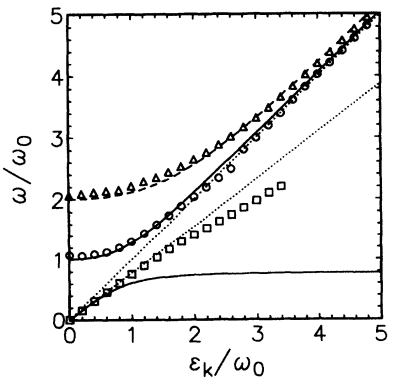

FIG. 1. Dispersion of the two independent boson modes for the coupling strength $\beta=0.1$ including the absolute values of the peak positions of Fig. 3. The lower solid line presents $\Omega_{k,1}$ and the upper one $\Omega_{k,2}$. The dotted lines indicate the small k behavior of $\Omega_{k,1}$ and the large k behavior of $\Omega_{k,2}$. For the dashed line see the text.

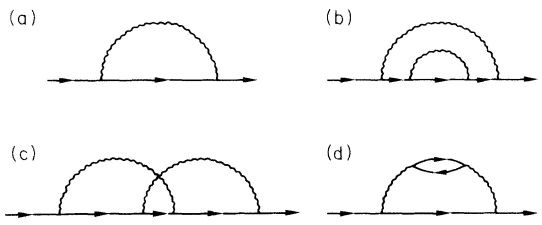

FIG. 2. Second and fourth order diagrams for the self-energy. The diagram 2(c) is the one neglected in the Migdal approximation.

Lehmann representation

$$\rho_+^<(k,\omega) = \sum_{\{n_{q,\nu}\}} A(\{n_{q,\nu}\})\delta\left(\omega + \sum_{q,\nu} n_{q,\nu}\Omega_{q,\nu}\right) \times \delta_{\tilde{k},\sum_{q,\nu} n_{q,\nu} q}, \quad (5)$$

where $A(\{n_{q,\nu}\})$ are the matrix elements with $n_{q,\nu}$ the boson occupation numbers, is helpful as in the case of the electron-electron interaction.[12] Simple explicit results for the matrix elements can be given for the g_4-type models.[12,14]

The threshold of the (unbroadened) spectral function $\rho_+^<(k_F + \tilde{k}, \omega)$ is determined by $n_{\tilde{k},1} = 1$, with all other $n_{q,\nu}$ zero, i.e., $\omega = -\Omega_{\tilde{k},1}$. The position of the main peak for $\tilde{k} \leq 0$ and $|\varepsilon_k| < \omega_0$ in Fig. 3 is given by this threshold energy. Increasing $|\varepsilon_k|$ this peak looses weight and broadens with the maximum approximately at $\tilde{v}_F\tilde{k}$ due to the decomposition of $\tilde{k}$ into many small negative momenta $\tilde{k}_i$ with $\Omega_{\tilde{k}_i,1} \approx \tilde{v}_F|\tilde{k}_i|$. Decompositions of $\tilde{k}$ involving at least one larger $|\tilde{k}_i|$ with energy $\Omega_{\tilde{k}_i,1}$ are responsible for the broadening. With increasing $|\varepsilon_k|$ the weight of the "first phonon satellite" at $\omega \approx -\Omega_{\tilde{k},2}$ increases and for $\varepsilon_k/\omega_0 \approx -2$ it has become the new "main peak." This exchange of peak character also occurs in the approximate spectral function Fig. 4 resulting from the second order self-energy calculation.[3] The main differences between the exact and approximate spectra are the power law asymmetry of the peak at threshold typical for Luttinger liquids and the more pronounced satellite structure in the exact solution. The power law behavior is due to decompositions of $\tilde{k}$ involving small *positive* $\tilde{k}_i$.[12] The nth order phonon satellite starts at $-n\omega_0$ for small $|\tilde{k}|$ and follows $-n\Omega_{\tilde{k}/n,2}$ for increasing $|\tilde{k}|$, which for $n = 2$ is shown as the dashed line in Fig. 1. The preference of this decomposition into n nearly equal momenta $\tilde{k}/n$ is a matrix element effect.[14] By increasing the coupling strength more and more satellites show up. For $|\varepsilon_{q_c}| \gg |\varepsilon_k| \gg \omega_0$ (not shown in Fig. 3) all these satellites end up in the remaining peak at $\omega = \varepsilon_k$, which also for the broadening $\gamma = 0$ has a finite width and resembles the Lorentzian of second order perturbation theory.[14]

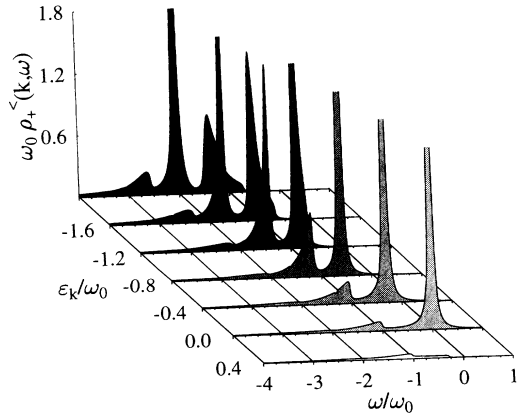

FIG. 3. Exact spectral function for the spinless model for $\beta = 0.1$. The broadening γ/ω_0 and $v_F\frac{2\pi}{L}/\omega_0$ are chosen 0.02.

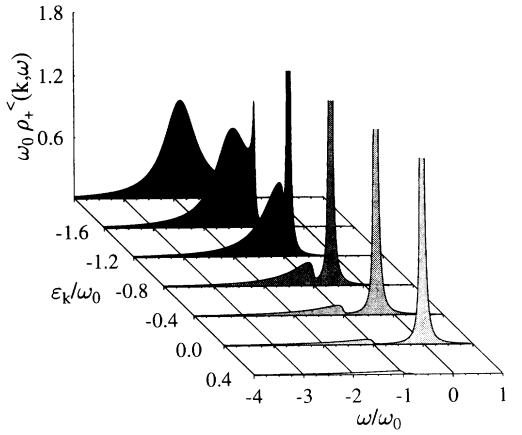

FIG. 4. Approximate spectral function following Ref. 3 for the same parameters as in Fig. 3.

For the model including electron spin the electron-phonon coupling term in Eq. (1) involves the *charge density*, while the spin degrees of freedom are not influenced by the phonons. The charge part of the Hamiltonian has the same form as in the spinless model but with the replacement $g(q) \to \sqrt{2}g(q)$. This implies for the Green's function $G_{\alpha,\sigma}^<(x,t)$ for the model including spin

$$iG_{+,\sigma}^<(x,t;g) = \left[iG_+^<(x,t;\sqrt{2}g)iG_+^<(x,t;0)\right]^{1/2}. \quad (6)$$

Results for the *same* $\tilde{g}$ value as used for the spinless model in Fig. 3, which corresponds to $\beta = 0.2$ for the coupling of the charge degrees of freedom, are shown in Fig. 5. The corresponding approximate spectral functions resulting from the second order self-energy are again presented by Fig. 4. In Fig. 5 the spin-charge separation of the threshold peak for $\tilde{k} < 0$ and $|\varepsilon_k| \leq \omega_0$ is the prominent feature. There are power law singularities determined by the anomalous dimension given in Eq. (4) at $\omega = \tilde{v}_F^c\tilde{k}$ and $\omega = v_F\tilde{k}$, where $\tilde{v}_F^c$ is the slope of $\Omega_{q,1}$ in the limit of small q. One should note that for small coupling the splitting between these peaks is of order $\tilde{g}^2$, but to obtain

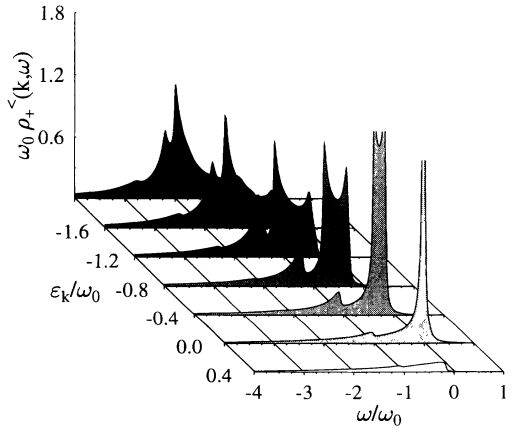

FIG. 5. Exact spectral function for the model including spin for the same parameters as in Fig. 3.

an indication of it in perturbation theory the calculation of all *fourth* order self-energy diagrams is necessary. For $|\varepsilon_k| \geq \omega_0$ the "spin peak" at $\omega = v_F\tilde{k}$ is the larger one and for increasing $|\tilde{k}|$ the "charge peak" decreases and gets broader as in the spinless case. Due to the second Green's function in the parentheses on the rhs of Eq. (6) the "spin peak" is at the "asymptotic" position $\omega = v_F\tilde{k}$ for *all* values of $\tilde{k}$. For $\varepsilon_k/\omega_0 \approx -2$ the peak that started out as the first phonon satellite for small $|\tilde{k}|$ has almost merged with the spin peak, in order to present the main peak. The behavior of the higher phonon satellites is similar to the spinless model. For $|\varepsilon_k| \approx \omega_0$ the difference between exact and approximate spectra is large, but increasing $|\varepsilon_k|$ it becomes smaller more quickly than in the spinless model, because of the "spin peak."

The results presented show that a reasonably strong coupling of the electrons to an Einstein mode in a quasi-one-dimensional conductor[17] has a strong influence on angular resolved photoemission spectra and with the energy resolution available[9] should be detectable. The detailed understanding of the electron-phonon interaction in 1D not only for weak coupling can be useful quite generally for systems where the electron-phonon coupling is large, e.g., doped C_{60} compounds.[18] A detailed presentation and interpretation of exact spectra also for a Debye model, inclusion of the electron-electron interaction, and the comparison with various approximations will be given elsewhere.[14]

[1] D. Langreth, Phys. Rev. B **1**, 471 (1971).

[2] For a review see C.O. Almbladh and L. Hedin, in *Handbook on Synchroton Radiation*, edited by E.E. Koch (North-Holland, Amsterdam, 1983), Vol. 1, p. 607.

[3] S. Engelsberg and J.R. Schrieffer, Phys. Rev. **131**, 993 (1963). Self-consistency is considered only with respect to the electron propagator.

[4] A.B. Migdal, Zh. Eksp. Teor. Fiz. **34**, 1438 (1958) [Sov. Phys. JETP **7**, 996 (1958)].

[5] A. Luther and I. Peschel, Phys. Rev. B **9**, 2911 (1974).

[6] F.D. Haldane, J. Phys. C **14**, 2585 (1981).

[7] I.E. Dzyaloshinskiĭ and A.I. Larkin, Zh. Eksp. Teor. Fiz. **65**, 411 (1973) [Sov. Phys. JETP **38**, 202 (1974)].

[8] M. Apostol and I. Baldea, Phys. Lett. A **88**, 73 (1982).

[9] B. Dardel *et al.*, Phys. Rev. Lett. **67**, 3144 (1991); B. Dardel *et al.*, Europhys. Lett. **24**, 687 (1993).

[10] G.M. Eliashberg, Zh. Eksp. Teor. Fiz. **38**, 966 (1960) [Sov. Phys. JETP **11**, 696 (1960)].

[11] V. Meden and K. Schönhammer, Phys. Rev. B **46**, 15 753 (1992).

[12] K. Schönhammer and V. Meden, Phys. Rev. B **47**, 16 205 (1993); B **48**, 11 390 (1993).

[13] J. Voit, Phys. Rev. B **47**, 6740 (1993); J. Phys. C **44**, 8305 (1993).

[14] V. Meden, K. Schönhammer, and O. Gunnarsson (unpublished).

[15] S. Tomonaga, Prog. Theor. Phys. **5**, 544 (1950).

[16] S. Engelsberg and B.B. Varga, Phys. Rev. **136**, A 1582 (1964). It is interesting to note that Engelsberg and Schrieffer (Ref. 3) have already discussed their results by using a model of coupled harmonic oscillators.

[17] R. Brusetti *et al.*, Phys. Rev. B **41**, 6315 (1990).

[18] O. Gunnarsson, V. Meden, and K. Schönhammer, this issue, Phys. Rev. B **50**, 10 462 (1994).

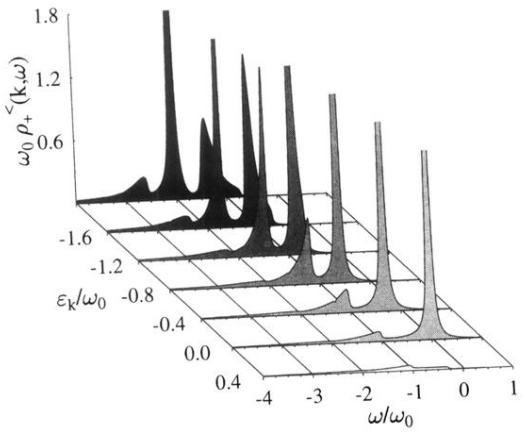

FIG. 3. Exact spectral function for the spinless model for $\beta = 0.1$. The broadening γ/ω_0 and $v_F \frac{2\pi}{L}/\omega_0$ are chosen 0.02.

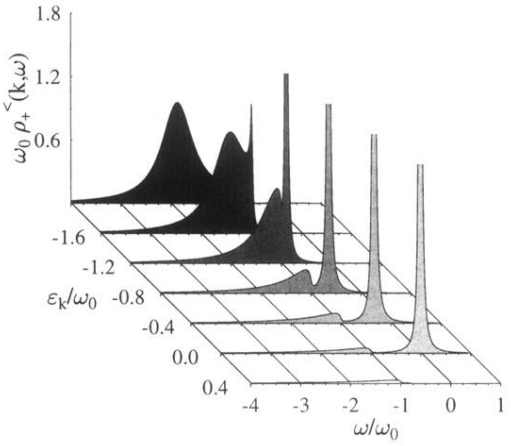

FIG. 4. Approximate spectral function following Ref. 3 for the same parameters as in Fig. 3.

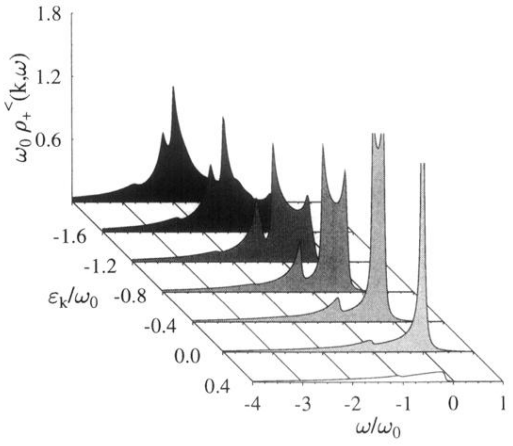

FIG. 5. Exact spectral function for the model including spin for the same parameters as in Fig. 3.